



Design of inhibitors of *Helicobacter pylori* glutamate racemase as selective antibacterial agents: Incorporation of imidazoles onto a core pyrazolopyrimidinedione scaffold to improve bioavailability

Gregory S. Basarab^{a,*}, Pamela Hill^a, Charles J. Eyermann^a, Madhu Gowravaram^a, Helena Käck^b, Ekundayo Osimoni^a

^a Infection Innovative Medicines, AstraZeneca R&D Boston, 35 Gatehouse Drive, Waltham, MA 02451, USA

^b AstraZeneca Discovery Sciences, Pepparedsleden 1, 431 83 Mölndal, Sweden

ARTICLE INFO

Article history:

Received 3 May 2012

Revised 28 June 2012

Accepted 2 July 2012

Available online 20 July 2012

Keywords:

Murl

Glutamate racemase

Helicobacter pylori

Antibacterial

Pyrazolopyrimidinedione

ABSTRACT

Structure–activity relationships are presented around a series of pyrazolopyrimidinediones that inhibit the growth of *Helicobacter pylori* by targeting glutamate racemase, an enzyme that provides D-glutamate for the construction of N-acetylglucosamine-N-acetylmuramic acid peptidoglycan subunits assimilated into the bacterial cell wall. Substituents on the inhibitor scaffold were varied to optimize target potency, antibacterial activity and in vivo pharmacokinetic stability. By incorporating an imidazole ring at the 7-position of the scaffold, high target potency was achieved due to a hydrogen bonding network that occurs between the 3-position nitrogen atom, a bridging water molecule and the side chains Ser152 and Trp244 of the enzyme. The lipophilicity of the scaffold series proved important for expression of antibacterial activity. Clearances in vitro and in vivo were monitored to identify compounds with improved plasma stability. The basicity of the imidazole may contribute to increased aqueous solubility at lower pH allowing for improved oral bioavailability.

© 2012 Elsevier Ltd. All rights reserved.

It is estimated that upwards of 50% of the world's population is infected with the Gram-negative bacterium *Helicobacter pylori*, a pathogen that colonizes the mucosal lining of the stomach.¹ Though many *H. pylori* infections are asymptomatic, they often lead to gastric disturbances such as ulcers and esophageal reflux and perhaps even to gastric cancer.² Currently a cocktail of three drugs including two broad-spectrum antibacterials is most often used over a two week period for the treatment of *H. pylori* infections, a treatment plagued by poor patient compliance due to diarrhea and other side effects resulting from the suppression of commensal bacteria. Furthermore, resistance of *H. pylori* to current therapies prompts the need for an alternative therapy with a new mode-of-action.^{1,3} For more severe and life-threatening infections, empiric therapy with broad-spectrum antibacterials constitutes the initial course of action due to the limited capabilities of determining the culpable pathogen in a timely fashion to tailor the choice of drug. However for the eradication of chronic, slow growing pathogens such as *H. pylori*, precise timing is less important and selectivity is desirable to eliminate the suppression of bacterial flora by broad-spectrum agents. The need for an improved therapy against *H. pylori* prompted our efforts to identify an orally active drug that operates by inhibition of glutamate racemase encoded

by the Murl gene essential for the biosynthesis of bacterial cell wall peptidoglycan. Murl is one of a series of genes responsible for building N-acetylglucosamine-N-acetylmuramic acid peptidoglycan subunits that are incorporated into the bacterial cell wall.⁴ D-glutamate (along with D-alanine and meso-diaminopimelic acid) is a necessary peptide component of bacterial peptidoglycan that confers a measure of proteolytic stability to the cell wall due to its atypical configuration. Deletion of Murl prevents peptidoglycan construction and bacterial viability by disrupting the supply of D-glutamate and thereby represents a worthwhile target for the design of antibacterial drugs.⁵ Comparative genomics showed a divergence for the Murl gene for *H. pylori* from other bacteria,⁶ both Gram-negative and Gram-positive, offering the expectation that a selective anti-*H. pylori* agent could be identified.

Figure 1 shows the structure for pyrazolopyrimidinedione inhibitor **1** of the *H. pylori* Murl isozyme that was discovered by high throughput screening against *H. pylori* Murl and of analogs **2** and **3** that were designed in subsequent analog optimization programs.^{6b,7} Compounds **1**, **2** and **3** show exquisite selectivity for the *H. pylori* Murl isozyme (IC₅₀s of 1400, 26 and 34 nM, respectively) relative to three other Murl isozymes (derived from *Staphylococcus aureus*, *Enterococcus faecalis* and *Escherichia coli*) where IC₅₀s exceeded the assay limit of 400 μM. The enzyme inhibitory potency translated into the suppression of *H. pylori* growth in vitro as the three compounds demonstrated MICs ranging from 0.5–8 μg/ml;

* Corresponding author. Tel.: +1 781 839 4689.

E-mail address: greg.basarab@astrazeneca.com (G.S. Basarab).

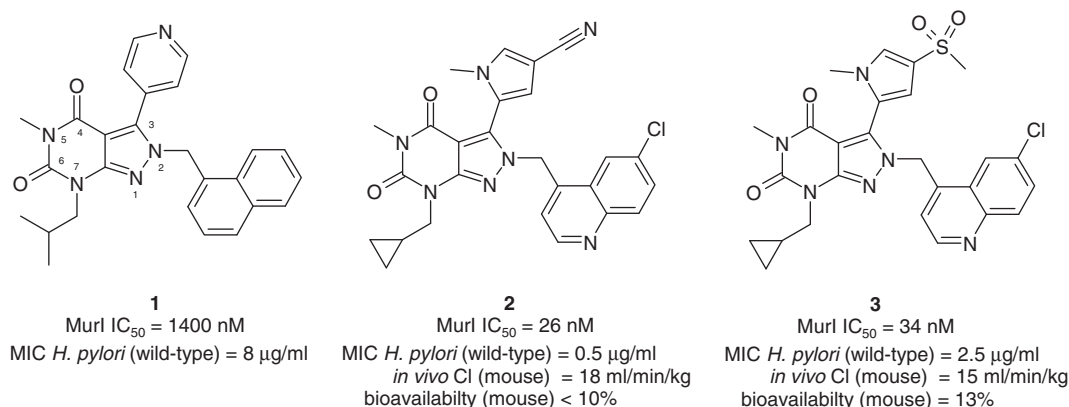


Figure 1. Biological properties of pyrazolopyrimidinedione inhibitors of glutamate racemase (MurI).

no MICs below the assay limit of 64 µg/ml were seen against a broad-spectrum of Gram-negative and Gram-positive pathogens.

As a practical matter, an anti-*H. pylori* therapy would be administered orally over a likely time course of treatment for 1–2 weeks.⁸ Therefore, the drug needs to achieve high blood levels by oral administration with sufficient exposure (after accounting for binding to endogenous protein) to exceed the MIC several fold over a period of time depending on the pharmacodynamic driver and magnitude. The free levels of **2** and **3** on oral dosing at 40 mg/kg in mouse models fell well below the MICs due, in large part, to low bioavailabilities. An exposure of **3** above its MIC = 2 could be maintained for 4 h by oral dosing 40 mg/kg of the pro-drug sulfoxide analog of **3**. However if the exposure is adjusted for the plasma protein binding (ppb of **3** is 97% in the mouse), the expectation is that the drug would not suppress *H. pylori* proliferation *in vivo*.⁷ We therefore set out to improve upon **2** and **3** by designing analogues with improved systemic exposure on oral dosing to the point that sustained free drugs levels well above MICs could be attained.

The x-ray derived crystal structure of **1** with the MurI enzyme^{6b} helped guide much of the inhibitor design strategies. Introducing polarity on the 2- and 7-position substituents (see Fig. 1 for numbering) is detrimental to inhibitory potency as both positions reside in hydrophobic environments of the enzyme binding pocket. By contrast, the 5-position extends along a hydrophobic surface that is exposed otherwise to solvent. The 3-position lies in a partially hydrophobic environment and a partially hydrophilic environment that extends out to solvent. The pyridine nitrogen of **1**, the nitrile of **2** and the sulfone of **3** lie within the hydrophilic region. Indeed, even more polar functionality such as sulfonamide and sulfoxide in place of the nitrile of **2** or the sulfone of **3** are well-tolerated for MurI inhibitory potency. However, polar substituents diminish bacterial membrane permeability resulting in higher MICs versus *H. pylori*.⁷ Indeed, a problem confounding design work is that hydrophobicity is best suited for membrane permeability and lower MICs while hydrophilicity oftentimes correlates with lower ppb and higher solubility that will translate into higher bioavailability properties that make for better drugs.

Chemistry

The 2-, 3-, 5- and 7-positions of the pyrazolopyrimidinedione scaffold can be systematically varied (see **1** for numbering) for developing structure–activity relationships via a single pot sequence that invokes two condensation reactions onto a pyrimidinedione hydrazide followed by a cyclization–rearrangement reaction as outlined in Scheme 1. Hydrazides **4** are condensed with 6-chloroquinoline-4-carboxaldehyde⁹ to form hydrazones **5**. Without isolation,

hydrazones **5** are condensed with a second aldehyde catalyzed by piperidine and heated to effect cyclization and rearrangement to compound **6** via a sequence first described by Yamada and co-workers and exemplified in the patent literature.¹⁰

The various hydrazides **4** are synthesized by methods set out in the literature wherein a monosubstituted urea is treated with diethylmalonate and base to form an intermediate pyrimidinetrione that is regioselectively converted to a pyrimidinedione chloride **7a** with POCl₃ (Scheme 2).^{6b,10,11} The NH of **7a** is alkylated on nitrogen leading to **8**. Alternatively, the 7-position substituent can be introduced first by alkylation of 6-chloro-1H-pyrimidine-2,4-dione to form **7b**; subsequent alkylation affixes the 5-position substituent. The chloride is then displaced with hydrazine to afford **4**.¹¹ Analogously, the compounds with the isobutyl substituent at the 7-position were made with isobutyl bromide in place of the cyclopropylmethyl bromide in the reaction sequences. Here we investigate the influence of 3- and 5-positions as opportunities to incorporate more polar functionalities deemed helpful for increasing solubility and improving physical properties that were, in turn, deemed important for bioavailability, clearance and plasma protein binding (ppb).

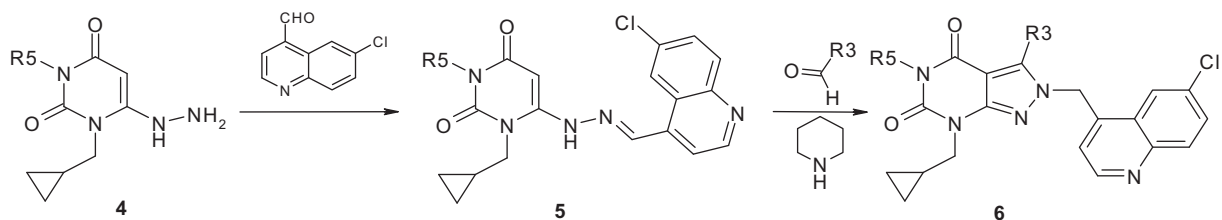
Many of the R³ aldehydes of Scheme 1 are commercially available or known in the literature while others required de novo synthesis.¹² The cyanoimidazole aldehyde **12** for incorporation into compounds **24** and **58–62** was prepared via sequence in Scheme 3. Initial protection of the starting imidazole carboxaldehyde was followed by dibromination to afford **10**. The bromine atom adjacent to the *N*-methylimidazole nitrogen was selectively removed by metal halogen exchange and quench with acid. Palladium catalyzed Zn(CN)₂ cross-coupling and hydrolysis affords **12**.

The cyanofuran aldehyde incorporated into **28** was prepared in 5 steps by the sequence outlined in Scheme 4. Reduction of ester **13** and protection of the alcohol to form **14** allows electrophilic cyanation with chlorosulfonyl isocyanate¹³ affording **15**. Deacylation and oxidation to the aldehyde finishes the sequence.

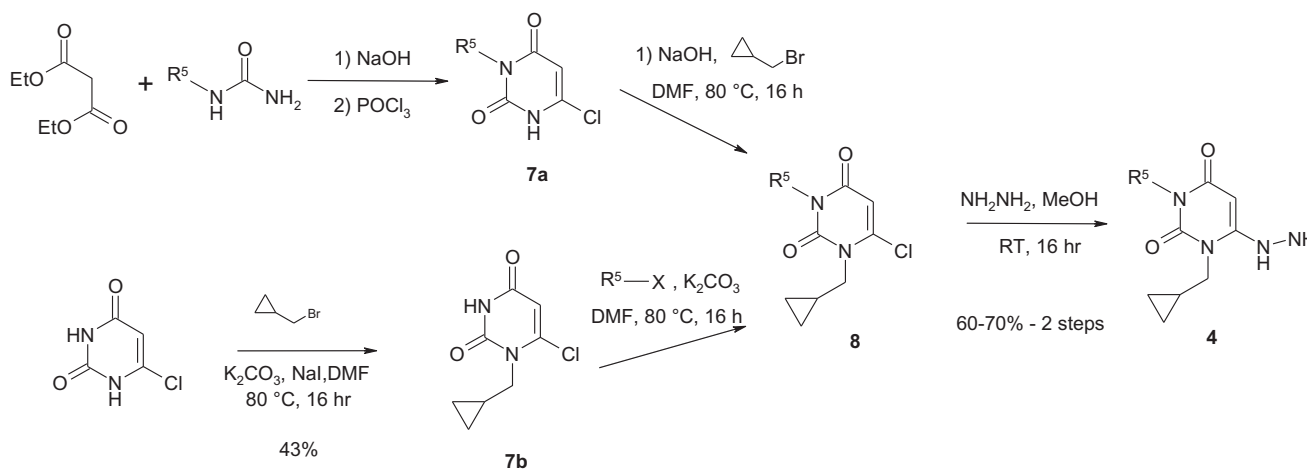
The isomeric cyanofuran aldehyde **20** for incorporation into **25** was prepared by an analogous sequence of steps (Scheme 5).

Results and discussion

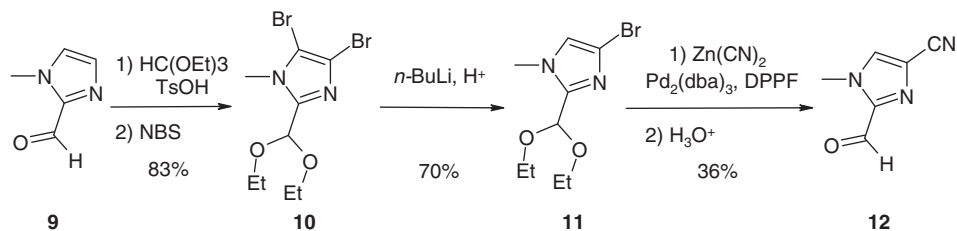
The cyclopropylmethyl substituent is optimal at the 7-position of the pyrazolopyrimidine scaffold as even a slight perturbation, the replacement of the cyclopropylmethyl group with an isobutyl group lowers potency 3-fold and leads to metabolically less stable compounds as determined by microsomal stability determinations. Compare compounds **2** and **23** with **26** and **27**, respectively (Table 1). Hence, the majority of the compounds described here were made with the 7-position cyclopropylmethyl substituent.



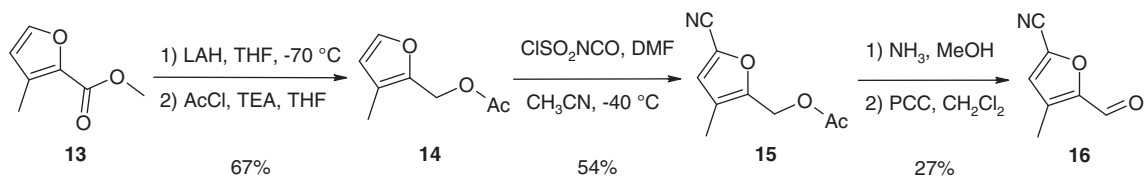
Scheme 1. General synthesis of the pyrazolopyrimidine scaffold.



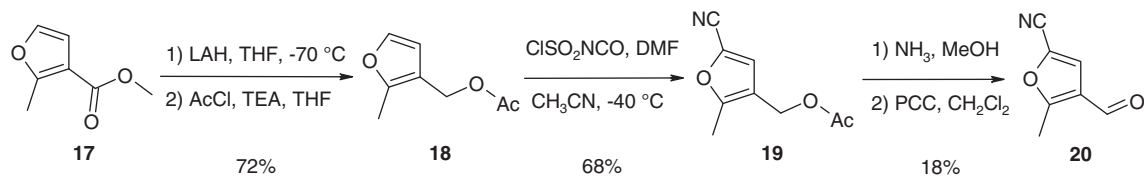
Scheme 2. General syntheses of key hydrazide intermediates **4** enabling variation of the R^5 substituent.



Scheme 3. Synthesis of cyanoimidazole **12** for construction of compounds **24** and **58–62**.



Scheme 4. Synthesis of cyanofuran **16** for construction of compound **28**.

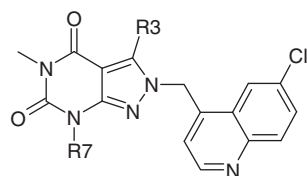


Scheme 5. Synthesis of cyanofuran **20** for construction of compound **25**.

Additionally, the chloroquinolinemethyl substituent at the 2-position is optimal^{6b} and was kept constant through the analogs herein. Enzyme bound compounds are likely pre-organized into

the binding conformation due to π - π stacking of the chloroquinoline with 3-position aromatic groups^{6b} leading to a hydrophobic collapse in aqueous solution.

Table 1
Influence of 3-position substituents on IC₅₀, MIC and Cl_{int}



Compd	R ⁷	R ³	IC ₅₀ (nM) ²⁰	MIC (μg/ml)		Cl _{int} ^c (μl/min/mg)	
				Wild type ^a	hefC ^{-b}	Human	Mouse
2			25	0.5	0.8	14	50
22			39	3	–	19	53
23			41	2	0.25	<17	21
24			87	4	2	<14	87
25			60	1	0.25	59	>100
26			86	4	–	94	>100
27			170	4	–	17	>100
28			220	2	2	38	63
29			220	8	–	20	>100
30			230	8	–	<14	64
31			260	18	–	>100	>100
32			280	8	–	34	>100
33			740	>32	–	<14	61
34			810	8	4	32	<14
35			900	32	–	92	>100

^a *H. pylori* strain 055.

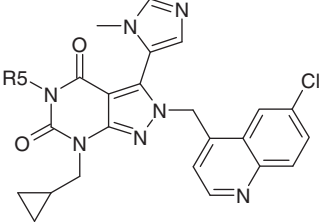
^b Ref. 14.

^c Liver microsome clearance.

Placing a 5-atom versus 6-atom aromatic heterocycle at the 3-position of the pyrazolopyrimidinedione scaffold affords the optimal inhibitory potency versus *H. pylori* Murl. Previous work had shown that potency is enhanced if there is a 1,3-orientation between the scaffold attachment and a polar group (e.g., sulfonamide) on the heterocycle.⁷ The polar group interacts directly or indirectly (through bridging water molecules) with hydroxyl of

Ser152, the indole NH of Trp244 and other hydrogen bonding residues that lie in the surrounding region of the enzyme in a channel that extends to solvent. However, the more polar functionality decreases antibacterial activity presumably due to lower membrane permeability. Previous work had also shown that a 1,2-orientation between the scaffold attachment and a small lipophilic group (methyl group or chlorine atom) improves inhibitory potency.⁷

Table 2
R³ Methylimidazoles: influence of 5-position substituents on IC₅₀'s, MICs and Cl_{int}



Compd	R ⁵	IC ₅₀ (nM) ²⁰	MIC (μg/ml)		Cl _{int} ^c (μl/min/kg)	
			Wild type ^a	hefC ^{-b}	Human	Mouse
36	HC≡CCH ₂ -	24	2	0.5	<14	18
37	HOCH ₂ C≡CCH ₂ -	54	64	16	>100	>100
38	CH ₂ =CHCH ₂ -	56	1	0.8	25	49
39		63	8	2	47	44
40		69	2	0.9	<14	44
41	CH ₃ CH ₂ -	72	4	1	<14	15
42		79	8	2	<14	6
43		170	64	16	>100	>100
44	(CH ₃) ₂ CH-	220	16	16	53	51
45	HC=C(CH ₃)CH-	460	8	8	21	65

^a *H. pylori* strain 055.

^b Ref. 14.

^c Liver microsome clearance.

The lipophilic group lies correspondingly in a complementary lipophilic pocket of the enzyme and enhances the staggered rotational conformation of the heterocycle relative to the scaffold. As might be expected, the increased potency along with increased lipophilicity enhancing membrane permeability improves antibacterial activity. In addition to MICs against a wild-type *H. pylori* strain, MICs are shown versus an *H. pylori* construct (designated *hefC*⁻) that is compromised by knock-out of the AcrB component of the AcrAB-TolC efflux pump machinery.¹⁴ This allows for interpretation of the contribution of permeation through the outer and inner membranes of the pathogen in limiting the expression of antimicrobial activities of the inhibitors.

So herein, we have incorporated a series of 5-membered ring heterocycles with a 1,3-orientation relative to the scaffold attachment for displaying a substituent towards the Ser152/Trp244 channel. A methyl group was additionally incorporated in a 1,2-orientation to the scaffold for an overall 1,2,4-orientation of methyl group, scaffold attachment, and substituent, respectively. The substituents of choice include those of intermediate polarity such as ketones and nitriles as well as the lone pair of a heterocyclic

nitrogen atom (the latter exemplified by **23** and **27**, Table 1 and the compounds of Table 2). A model derived by x-ray diffraction of crystals of a complex of **21** with the enzyme (Fig. 2) shows the imidazole lone pair of electrons associated with a water molecule that is positioned to bridge Ser152 and Trp244 in a hydrogen bonding array.¹⁵ Compound **21** was one of the first compounds made in this series and has the non-optimized isobutyl group at the 7-position and a non-optimized naphthylmethyl substituent at the 2-position. Positioning a carbon atom with a hydrogen substituent instead of the imidazole lone pair of electrons towards this region as in pyrrole **31**, triazole **34**, and imidazole **35** confers considerably lower potency. The small amino substituent of **32** and **33** is also detrimental to activity. Slightly larger substituents such as the nitrile, by contrast, dislodge the bringing water molecule and can form direct interactions with the enzyme, hence accounting for the better potencies that must be attributed in part to the overall entropy gain. Examples of a nitrile displacing a crystallographic water molecule to increase inhibitory potency have been documented.¹⁶ Decreased inhibitor potency was seen if a heteroatom is placed in any of the other positions of the heterocycle as exemplified by comparing **23**–**30** where the transformation from imidazole to triazole decreases inhibitory potency 7 to 8-fold. Cyanoimidazole **24** shows decreased potency (2 to 3-fold) relative to cyanopyrrole **2** as do cyanofurans **25** and **28** (2- and 8-fold, respectively). However, due to the lipophilic nature of the cyanoheterocycles, membrane permeability is increased and antimicrobial activity does not deteriorate correspondingly.

Maintaining the better heterocycles at the 3-position (imidazole, cyanopyrrole and cyanoimidazole, Tables 2 and 3) allows elaboration of the scaffold 5-position to further explore structure–activity insights. As mentioned, the 5-position abuts a hydrophobic patch and otherwise opens to bulk solvent (Fig. 2). Hence, both lipophilic and polar groups can be tolerated in this position, though in line with previous observations, higher polarity compromises MICs even when potencies are only reduced a few fold (compare **37** and **43** with **23**, for example). Compound **46** registers one of the higher inhibitory potencies against the Murl enzyme, yet MICs are higher due to the polar triazole group. Similarly, the MICs of **48**–**50** trend upward due to the polar substituents. Oftentimes, much better MICs are recorded for the more polar compounds against the pump debilitated *hefC*⁻ strain of *H. pylori*. This is particularly evident from previous work in which particularly polar sulfonamide and sulfoxide substituents afforded efflux ratios (the ratio between the MIC of wild-type *H. pylori* and the *hefC*⁻ strain) of 32–64 or more and resulted with exceedingly high MICs versus the wild-type strain.⁷ Consequently, much of the work herein focussed on less polar substituents in compound design. A working hypothesis that drives the design is that the efflux pump recognizes the various more polar and less polar compounds somewhat equally, and therefore, elimination of the pump would lead to a more pronounced lowering of MICs for more polar compounds with the reduced capability to cross bacterial membranes. More

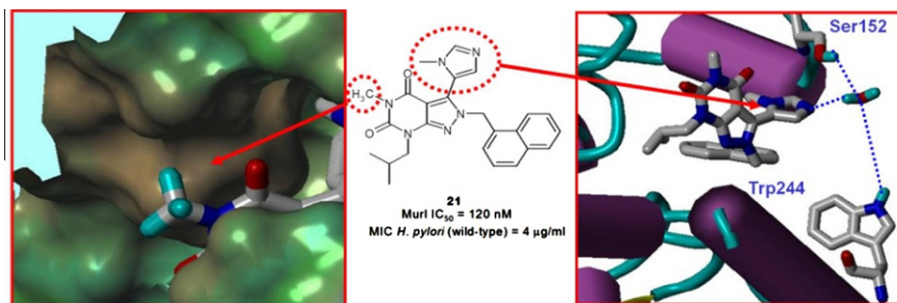
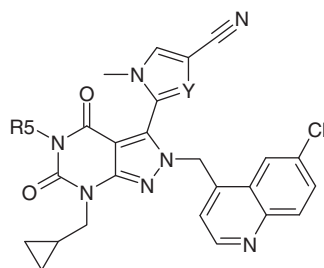


Figure 2. Surface surrounding 5-position substituent (left) and H-bonding array with a crystallographic water molecule, Ser152 and Trp244 (right).

Table 3
R³ Cyanopyrroles and cyanoimidazoles: influence of 5-position substitution



Compd	R ⁵	Y	IC ₅₀ (nM) ²⁰	MIC (μg/ml)		Cl _{int} ^c (μl/min/mg)	
				Wild Type ^a	hefC ^{-b}	Human	Mouse
46		CH	13	8	16	>100	>100
47	HC≡CCH ₂ -	CH	28	0.75	0.3	<14	16
48		CH	51	16	4	>100	>100
49	NCCH ₂ -	CH	55	8	1	<14	96
50	HOCH ₂ C≡CCH ₂ -	CH	57	32	16	>100	>100
51		CH	62	2	2	23	<14
52	CH ₃ CH ₂ -	CH	70	0.75	0.6	25	17
53	CH ₂ =CHCH ₂ -	CH	70	1.5	1	33	76
54	CH ₃ C≡CCH ₂ -	CH	74	2	2	99	>100
55		CH	80	2	0.13	30	33
56	HOCH ₂ CH ₂	CH	88	64	16	>100	>100
57		CH	120	8	4	>100	>100
58	HC=C(CH ₃)CH-	CH	160	2	8	91	>100
59	(CH ₃) ₂ CH-	CH	240	4	8	26	>100
60		CH	260	64	4	41	>100
61		CH	470	32	32	>100	>100
62		CH	670	16	16	>100	>100
63	HC≡CCH ₂	N	89	1	2	<14	28
64		N	150	2	2	ND	ND
65	CH ₃ CH ₂	N	180	2	2	51	<14
66	CH ₂ =CHCH ₂	N	250	2	4	>100	>100
67		N	250	8	4	<14	<14

^a *H. pylori* strain 055.

^b Ref. 14.

^c Liver microsome clearance.²¹

lipophilic methyl, ethyl, cyclopropyl, cyclopropylmethyl, allyl and propargyl R³ substituents are favored for wild-type MICs. Indeed, the efflux ratios of compounds are about two or less (compounds **2**, **28**, **38**, **40**, **44–45**, **47**, **51–54**, **58–59**, and **63–66**) with more lipophilic functionality. Recognizing that the individual MICs can have a 2-fold variations, the trend holds that efflux ratios increase with greater polarity and decrease with greater lipophilicity, though subtle exceptions to the observations may be seen. Branching at

the attachment point of the R⁵ substituent reduces inhibitory potency as seen with the incorporation of isopropyl groups of **44** and **59** and α -methyl propargyl groups of **45** and **58**. The reduction in binding potency is less pronounced (about 3-fold) for the cyclopropyl substituent seen in **37**, **51** and **64** relative to the methyl substituent of **23**, **2** and **24**, respectively.

Mouse and human microsomal clearances were determined in parallel with MICs; compounds with lower MICs and Cl_{int} values

Table 4
PK parameters in the mouse²²

	Compound 23	Compound 36
Cl (ml/min/kg)	14	20
t _{1/2} (h)	0.7	2.1
V _{ss} (L/kg)	1.2	3.6
F (%)	76	100
ppb ²³	<3.1	4

less than 50 ml/min/mg were evaluated in vivo for PK characteristics in the mouse. The highest drug exposure (AUC on oral dosing of 40 mg/kg of drug) was recorded by the compounds where R⁷ = imidazole; in particular, **23** and **36** (Table 4) exhibit lower clearances and higher bioavailabilities combined to give sustained blood levels that rise well above the MICs as exemplified with the time course plot for **36** in Chart 1. The improvement in bioavailability with the imidazole is believed to relate to its weak basicity enhancing solubilization in the acidic conditions of the stomach before passing to the intestine for absorption. The pK_a of the **36** was measured to be 7.2 in line with the weakly basic imidazole substituent.

Compound **36** was tested for efficacy in a murine *H. pylori* infection model dosing for 2 days post inoculation at 40 mg/kg qid, in part to determine the pharmacodynamic (PD) driver. A modest, statistically insignificant 1 log reduction in the CFU count versus the untreated control was seen despite achieving blood levels 4X the MIC. As a positive control, Y-34867, a fluoroquinolone with anti-*H. pylori* activity,¹⁷ was dosed for 2 days at 10 mg/kg bid showing complete eradication of the pathogen (nearly 5 log reduction in CFU counts). The reasons for the compound failing in the efficacy experiment are many-fold. A more potent drug in this class with a higher free fraction would be better suited for showing eradication of *H. pylori* in the model as a test in principle whether Murl inhibition would be a viable mode-of-action in vivo. This would hold in particular if the PD driver were AUC/MIC or C_{max}/MIC versus Time/MIC, the latter being less sensitive to protein binding effects. Unfortunately, the efficacy experiment with **36** falls short of being able to delineate the PD driver that would aid future compound design. Additionally, it would be of interest to determine whether the blood levels of drug correlate with levels that might meet the stomach region of colonization. *H. pylori* is a relatively slow growing pathogen that evades the body's immune system colonizing the stomach mucosa for years or decades. A compound with cidal activity is best suited in such a situation,¹⁸ and the class of compounds described herein is static.¹⁹ The question arises as to whether the target site is limiting towards achieving cidal activity or the whether the pyrazolopyrimidine class of inhibitors is not cidal in itself; additional work is needed to improve the understanding.

In summary, progress was made towards achieving good PK properties (clearance and bioavailability) for the pyrazolopyrimidine class of compounds that inhibit the growth of *H. pylori* by

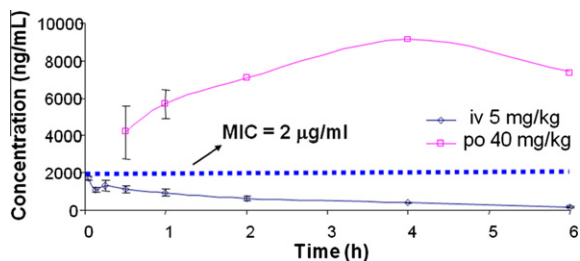


Chart 1. Mouse PK of compound **36**.

incorporating an imidazole ring at the 7-position of scaffold. The imidazole was shown to impart higher target potency through a hydrogen bonding network with a bridging water molecule to the protein. The basicity of the imidazole may also contribute to increased aqueous solubility that allows for improved adsorption. Adjustment of substituents otherwise help to optimize target potency, antibacterial activity and in vivo stability. However, more work needs to be done to understand the limiting factors for translation to good efficacy in an animal model and for utility as a therapy for treatment of *H. pylori* infections in humans.

Acknowledgments

Credit should be given to Tomas Lundqvist of AstraZeneca Discovery Sciences for assistance in generating the crystal structure of the Murl enzyme–inhibitor complex. The AstraZeneca Infection Innovative Medicines Biosciences Department determined the MICs and carried out the in vivo efficacy studies. The AstraZeneca Infection Innovative Medicines DMPK group performed the in vitro and in vivo PK assessments.

References and notes

- Jones, K. R.; Cha, J.-H.; Merrell, D. S. *Curr. Drug Ther.* **2008**, *3*, 190.
- (a) Malfertheiner, P.; Bornschein, J.; Selgrad, M. J. *Digestive Dis.* **2010**, *11*, 2; (b) Kim, S. S.; Ruiz, V. E.; Carroll, J. D.; Moss, S. F. *Cancer Lett.* **2011**, *305*, 228.
- (a) O'Connor, A.; Gisbert, J. P.; McNamara, D.; O'Morain, C. *Helicobacter* **2010**, *15*, 46; (b) Graham, D. Y.; Fischbach, L. *Gut* **2010**, *59*, 1143; (c) Suzuki, H.; Nishizawa, T.; Hibi, T. *Future Microb.* **2010**, *5*, 639.
- (a) Van Heijenoort, J. *J. Nat. Prod. Rep.* **2001**, *18*, 503; (b) Doublet, P.; van Heijenoort, J.; Mengin-Lecreulx, D. *J. Bacteriol.* **1992**, *174*, 5772; (c) Glavas, S.; Tanner, M. E. *Biochemistry* **2001**, *40*, 6199; (d) Doublet, P.; van Heijenoort, J.; Mengin-Lecreulx, D. *Biochemistry* **1994**, *33*, 5285.
- Fisher, S. L. *Microbiol. Biotechnol.* **2008**, *1*, 345.
- (a) Supuran, C. T. *Future Microbiol.* **2007**, *2*, 111; (b) Lundqvist, T.; Fisher, S. L.; Kern, G.; Folmer, R. H. A.; Xue, Y.; Newton, D. T.; Keating, T. A.; Alm, R. A.; de Jonge, B. L. M. *Nature* **2007**, *447*, 817; (c) Doig, P.; de Jonge, B. L.; Alm, R. A.; Brown, E. D.; Uria-Nickelsen, M.; Noonan, B.; Mills, S. D.; Tummino, P.; Carmel, G.; Guild, B. C.; Moir, D. T.; Vovis, G. F.; Trust, T. J. *Microbiol. Mol. Biol. Rev.* **1999**, *63*, 675.
- Basarab, G. S.; Hill, P.; Rastagar, A.; Webb, P. H. *J. Bioorg. Med. Chem. Lett.* **2008**, *18*, 4716.
- Graham, D. Y.; Lu, H.; Yamaoka, Y. *Curr. Opin. Drugs* **2008**, *68*, 725.
- Campbell, K. N.; Sommers, A. H.; Kerwin, J. F.; Campbell, B. K. *J. Am. Chem. Soc.* **1946**, *68*, 1851.
- (a) Yamada, F. *J. Am. Chem. Soc.* **1974**, *96*, 5607; (b) Basarab, G.; Eyermann, J.; Gowravaram, M.; Green, O.; MacPherson, L.; Morningstar, M.; Nguyen, T. U.S. Patent 7285558, 2004; *Chem. Abstr.* **2004**, *139*, 89821; (c) Cheshire, D.; Cooper, M.; Donald, D.; Thorne, P. U.S. Patent, 2000, 6028074; *Chem. Abstr.* **2000**, *129*, 302556.
- (a) Naka, T.; Furukawa, Y. *Chem. Pharm. Bull.* **1979**, *6*, 1328; (b) Isobe, Y.; Hirota, K. *Chem. Pharm. Bull.* **2003**, *12*, 1451.
- The corresponding aldehydes for formation of the 3-position substituents in compounds **17**, **18**, **23** and **26–40** are commercially available. The synthesis of the aldehyde for the formation of the 3-position substituents of compounds **21**, **41–57** is described in: Loader, C. E.; Anderson, H. J. *Can. J. Chem.* **1981**, *59*, 2673 and Ref. 10b. The synthesis of the corresponding aldehyde for the formation of the 3-position substituent of compounds **25** is described in: Moderhack, D.; Hoppe-Tichy, T. *J. Prakt. Chem., Chem. Zeit.* **1996**, *338*, 169 and Ref. 10b.
- Floyd, A. J.; Kinsman, R. G.; Roshan-Ali, Y.; Brown, D. W. *Tetrahedron* **1983**, *39*, 3881.
- (a) de Jonge, B. L. M.; Kutschke, A.; Uria-Nickelsen, M.; Kamp, H. D.; Mills, S. D. *Antimicrob. Agents Chemother.* **2009**, *53*, 3331; (b) Kutschke, A.; de Jonge, B. L. M. *Antimicrob. Agents Chemother.* **2005**, *7*, 3009.
- Crystallization of compound **21** with Murl was carried out as described in Ref. 6b. The data and coordinates are deposited in the Protein Data Bank; the accession code is 4b1f.
- (a) Chen, J. M.; Xu, S. L.; Wawrzak, Z.; Basarab, G. S.; Jordan, D. B. *Biochemistry* **1998**, *37*, 17735; (b) Liu, C.; Wroblewski, S. T.; Lin, J.; Ahmed, G.; Metzger, A.; Wityak, J.; Gillooly, K. M.; Shuster, D. J.; McIntyre, K. W.; Pitt, S.; Shen, D. R.; Zhang, R. F.; Zhang, H.; Doweiko, A. M.; Diller, D.; Henderson, I.; Barrish, J. C.; Dodd, J. H.; Schieven, G. L.; Leftheris, K. *J. Med. Chem.* **2005**, *48*, 6261.
- Sakurai, N.; Sano, M.; Hirayama, F.; Kuroda, T.; Uemori, S.; Moriguchi, A.; Yamamoto, K.; Ikeda, Y.; Kawakita, T. *Bioorg. Med. Chem. Lett.* **1998**, *8*, 2185.
- (a) Suzuki, H.; Nishizawa, T.; Hibi, T. *Future Microbiol.* **2010**, *5*, 639; (b) Gisbert, J. P.; Calvet, X.; O'Connor, J. P. A.; Megraud, F.; O'Morain, C. A. *Exp. Opin. Pharmacother.* **2010**, *11*, 905.

19. Unpublished work, B.M.L. de Jonge, AstraZeneca Infection Innovative Medicines.
20. IC_{50} is the mean of duplicate determinations by the method in Ref. 6b. Murl protein was expressed from murl gene of chromosomal DNA of wild-type *Helicobacter pylori* strain J 99 (human isolate, Tenn. Genome Therapeutic Corporation, now Oscient Pharmaceuticals, Inc.)
21. Metabolic stability was determined by incubating a 2 μ M compound solution in 0.5 mg/ml human or mouse microsomes and adding 1 mM NADPH. Compound concentrations at different time points were quantified by LC/MS. Intrinsic clearance (Cl_{int}) was calculated from disappearance of the compound.
22. Compounds for oral and iv dosing in mice were formulated in 25% PEG/water and 4:4:2 dimethylacetamide-PEG400–water, respectively. Compound concentrations in plasma at different time points were quantified by LC/MS. Pharmacokinetic (PK) parameters were calculated by using WinNonlin. Mean results were determined from experiments run in triplicate.
23. Plasma protein binding (ppb) was determined from a 10 μ M compound solution in a Dianorm plasma well incubating at 37 °C for 16 h. Free fractions were calculated from ratio between drug concentration in buffer and drug concentration in buffer plus plasma wells as determined by LC/MS.